

## Numerical study of car radiator using dimple roughness and nanofluid

ROBIN KUMAR THAPA<sup>a</sup>  
VIJAY SINGH BISHT<sup>a</sup>  
PRABHAKAR BHANDARI<sup>b\*</sup>  
KAMAL SINGH RAWAT<sup>c</sup>

<sup>a</sup> Uttarakhand Technical University, Faculty of Technology, Chakrata Road, Dehradun-248007, Uttarakhand, India

<sup>b</sup> K.R. Mangalam University, Mechanical Engineering Department, Sohna Road, Gurgram-122103, Haryana, India

<sup>c</sup> MIET, Mechanical Engineering Department, Meerut-250005, Uttar Pradesh, India

**Abstract** Thermal augmentation in flat tube of car radiator using different nanofluids has been performed more often, but use of artificial roughness has been seldom done. Artificial roughness in the form of dimple is used in the present research work. Present study shows the impact of dimple shaped roughness and nanofluid ( $\text{Al}_2\text{O}_3$ /pure water) on the performance of car radiator. The pitch of dimples is kept at 15 mm (constant) for all the studies performed. The Reynolds number of the flow is selected in the turbulent regime ranging from 9350 to 23000 and the concentration of the nanofluid is taken in the range of 0.1–1%. It has been found that the heat transfer rate has improved significantly in dimpled radiator tube on the expense of pumping power. Furthermore, the heat transfer rate also increases with increase in nanoparticle concentration from 0.1% to 1.0%. The highest heat transfer enhancement of 79% is observed at Reynolds number 9350, while least enhancement of 18% is observed for Reynolds number of 23000.

**Keywords:** Heat transfer augmentation; Nanofluid; Pumping power; Car radiator; Artificial roughness

---

\*Corresponding Author. Email: [prabhakar.bhandari40@gmail.com](mailto:prabhakar.bhandari40@gmail.com)

## Nomenclature

$A_p$	–	heat transfer area, mm <sup>2</sup>
$A_t$	–	cross sectional area of flat tube, mm <sup>2</sup>
$C$	–	correction factor
$C_p$	–	heat capacity, J/kgK
$d_h$	–	hydraulic diameter, mm
$d_p$	–	particle diameter, mm
$h_{nf}$	–	heat transfer coefficient, W/m <sup>2</sup> K
$K$	–	thermal conductivity, W/m·K
Nu	–	Nusselt number
Re	–	Reynolds number
$T_b$	–	bulk temperature, K
$T_{in}$	–	inlet temperature, K
$T_{out}$	–	outlet temperature, K
$T_w$	–	average wall temperature of flat tube, K
$\vec{u}$	–	velocity vector
$V_t$	–	velocity at the inlet of flat tube, m/s
$y^+$	–	dimensionless distance from the wall
$\Delta p$	–	pressure drop, N/m <sup>2</sup>

## Greek symbols

$\delta$	–	distance between the nanoparticles, nm
$\mu$	–	dynamic viscosity, kg/m·s
$\rho$	–	density, kg/m <sup>3</sup>
$\Phi$	–	empirical shape factor
$\Psi$	–	particle sphericity of nanoparticle

## Subscripts

bf	–	base fluid
nf	–	nanofluid
$p$	–	nanoparticle

## 1 Introduction

In automotive market, there is a huge demand for more powerful engines with aesthetic car design. The design department has to go through multiple challenges in doing so. One of the major problems is the dissipation of the waste heat produced by engines (about one third of total heat) through cooling system. Rejection of this waste heat should be very effectively otherwise it may lead to increase in pollution, fuel consumption and even damage the engine components. With the increase in engine power, the size radi-

ator also increases to dissipate extra waste heat. However, increasing the size of the radiator will lead to major design changes. This problem can be resolved by increasing the efficiency of cooling systems without changing the size of the radiator. The efficiency of cooling system can be enhanced by using active and passive methods. However, active method required external power. An efficient cooling system can decrease fuel consumption and helps to improve the engine performance [1].

The performance of cooling system can be enhanced by using various heat transfer enhancement techniques *viz.* effective geometry, modified coolant, increase surface area, etc. Apart from that use of fins and various design of microchannels are other ways to improve the performance [2]. Initially, Water was used as a working fluid to extract heat, however due to its freezing point limitation now mixture of water and some freezing point depressants are used. Weight fraction of freezing point depressant in working fluid depends upon the local weather conditions. However, use of freezing point depressant also affects the thermal conductivity of the working fluid [3]. The thermal characteristics of working fluid can be augmented by introducing nanoparticles. The use of nanofluids as a working fluid in engine cooling system has gain huge attention of researchers [4].

Choi and Eastman were the first to show the use of nanofluids by using metal and metals oxides as suspended nanoparticles in base fluid [5]. Various researchers used the nanofluids to enhance the thermal performance of the car radiator. Ahmed *et al.* [6] investigated the thermal performance of the car radiator with  $\text{TiO}_2$ -water nanofluids for the laminar flow regime. They concluded that performance of the car radiator is optimum with 0.2% concentration of  $\text{TiO}_2$ -water nanofluid. Naraki *et al.* [7] investigated effect of  $\text{CuO}$ -water nanofluid on heat transfer in a car radiator and concluded that, heat transfer significantly increased with the use of nanofluid. Apart from that they also reported heat transfer rate increase with nanoparticles concentration and decrease with temperature. Heris *et al.* [8] also investigated thermal performance of  $\text{CuO}$  nanoparticles with water and ethylene glycol mixture and reported that Nusselt number increased with increase of Reynolds number and nanoparticle concentration.  $\text{SiO}_2$  based and  $\text{ZnO}$  based nanofluid was also used in car radiator and enhancement of 13.9% and 16% was observed in car radiator effectiveness, respectively [9]. Various researchers also used  $\text{Al}_2\text{O}_3$  based nanofluids in automobile radiator to enhance the thermal performance [10–13]. Senthilraja *et al.* [14] compare the performance of a radiator using  $\text{CuO}$  and  $\text{Al}_2\text{O}_3$  based nanofluids and concluded that  $\text{CuO}$  based nanofluid performed better heat transfer

compared to  $\text{Al}_2\text{O}_3$  based nanofluids. Furthermore, researchers also studied effect of various types of inserts along with nanofluids on the thermal performance of radiator. Chougule *et al.* [15] experimentally investigated effect of wire coil insert with nanofluid in a circular tube. They observe augmented thermal performance for low volume concentration of CNT/water nanofluid. Recently, Singh *et al.* [16,17] has proposed dimple and protrusion in conical insert inside of heat exchanger for enhancing the performance. Kore *et al.* [18] performs numerical study on rectangular channel having variable dimple depth and pointed out that with increase in dimple depth, heat transfer rate firstly increases and then after certain dimple depth it decreases. Katkhaw *et al.* [19] studies the inline and staggered arrangement of dimples over heated surface and proposes correlations for both the arrangement. Various materials has been opted in car radiators and erosion parameters should also be considered while selecting proper material [20, 21].

Most of the studies have been focused on passive techniques and used various insert [22,23] and different nanofluids [24–26]. However, heat transfer augmentation in flat tube of car radiator using different nanofluids has been performed very often. Apart from that use of artificial roughness has been seldom done. Therefore, in the present work computational study of roughened automobile radiator tubes with  $\text{Al}_2\text{O}_3$  based nanofluid has been performed.

## 2 Numerical modelling

### 2.1 Physical model and governing equations

The complete schematic diagram of car radiator is shown in Fig. 1a. It consists of series of flat tubes since they offer low resistance to surrounding air in comparison circular cross-section tubes. The horizontal fins are present between the vertical flat tubes. However, to reduce the computational cost and time, in the present work only single flat tube is considered and furthermore simulation has been performed for vertically halved portion to take the advantage of symmetry in the model as shown in figure. Figure 1b shows half of the single flat tube simulated in this study with specifications. The length of the flat tube is 310 mm. The width and height of the flat tube's cross-section is 3 mm and 20 mm, respectively. The ribs were wrapped all around the inside wetted face of the flat tube. There were total 60 dimples in tube placed at a pitch of 15 mm as shown in Fig. 2a.

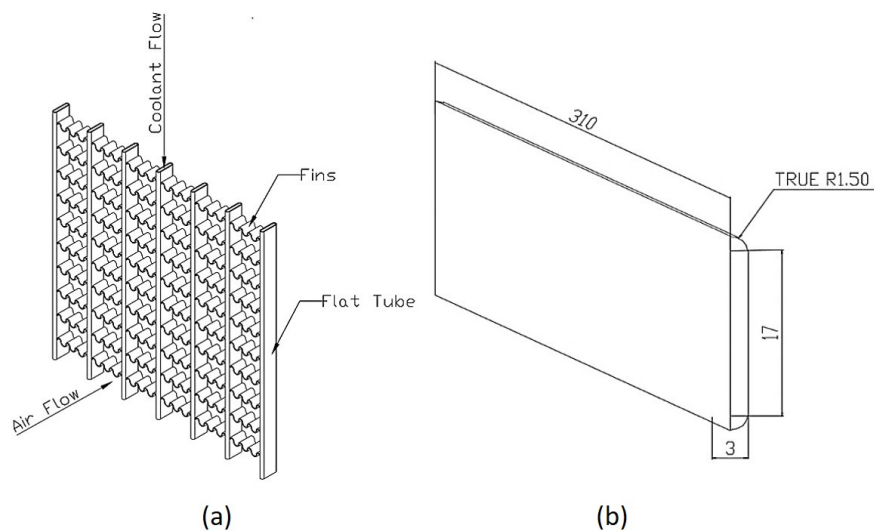


Figure 1: (a) Actual model of the car radiator. (b) Computational domain of single flat radiator tube (axis symmetric view).

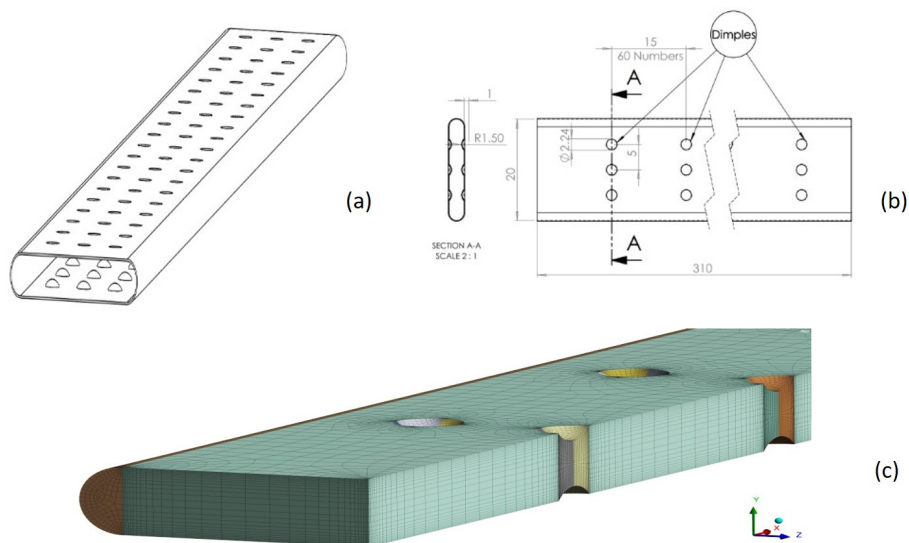


Figure 2: Dimpled flat tube configuration: (a) isometric view, (b) side and top view with specification, (c) meshed view.

The thermophysical properties of nanofluid, i.e. density, specific heat, thermal conductivity, and viscosity were obtained using following expressions:

Density of nanofluid has been calculated by the expression given by Pak and Cho [27]

$$\rho_{nf} = \Phi \rho_p + (1 - \Phi) \rho_{bf}. \quad (1)$$

Specific heat capacity of nanofluid was evaluated from the expression by Xuan and Roetzel [28]

$$Cp_{nf} = \frac{\Phi \rho_p Cp_p + (1 - \Phi) \rho_{bf} Cp_{bf}}{\rho_{nf}}, \quad (2)$$

while thermal conductivity has been calculated by Hamilton model [29]

$$k_{nf} = \frac{k_p + (\Phi - 1)k_{bf} - \Phi(\Phi - 1)(k_{bf} - k_p)}{k_p + (\Phi - 1)k_{bf} + \Phi(k_{bf} - k_p)}, \quad (3)$$

where  $\Phi$  is empirical shape factor given by  $\Phi = 3/\Psi$ .  $\Psi$  is the particle sphericity of nanoparticle which is measured as the ratio of surface area of a sphere that has same volume as the nanoparticle to the actual surface area of the nanoparticle. Since the shape of the particle considered in this study is spherical therefore the particle sphericity will come out to be 1. Hence the empirical shape factor considered in this study is 3.

The effective viscosity of nanofluid has been determined by Masoumi *et al.* [30]

$$\mu_{nf} = \mu_{bf} + \frac{\rho_p V_B d_p^2}{72C\delta}, \quad (4)$$

where  $V_B$  is the Brownian motion velocity.

## 2.2 Meshing and grid independence test

For both the configurations, i.e. plain and dimpled radiator, a high-quality grid was generated using the slicing technique in ANSYS meshing application [31]. The generated mesh for the dimpled configurations is shown in Fig. 2c. The orthogonal quality was maintained above 0.3 and the skewness was maintained below 0.77. Small sized elements were created in the region of high gradients, i.e. near the walls and ribs. The grid comprised of hexahedral and wedge shaped elements. The near wall treatment used in this study was enhanced wall treatment in which the mesh was resolved up to the viscous sublayer. To achieve this fine mesh, the wall  $y^+$  (dimensionless

distance from the wall) was kept below 5 to ensure that the first element from the wall lies within the viscous sublayer. The cell wall distance for  $y^+ = 5$  was calculated for the case with maximum Reynolds number, i.e. 23 000. Inflation layer was created around the walls to capture the boundary layer and important feature of the flow. Figure 3 shows the variation of Nusselt number with number of elements for  $Re = 9350$  for flat radiator tube. Total of five different cases has been considered in the grid independence test. It has been observed that last two grids has shown less than 1% variation in Nusselt number, so grid size having 525 605 number of elements has been used in further study.

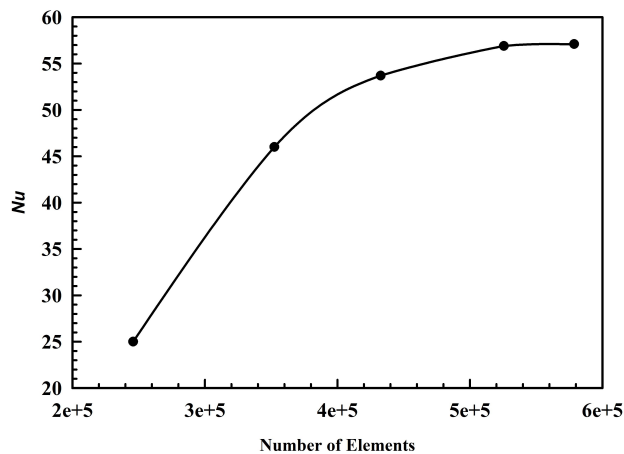


Figure 3: Variation of Nusselt number in flat radiator tube with number of elements for  $Re = 9350$ .

### 2.3 Numerical procedure

The present work has been carried out in commercial computational fluid dynamics (CFD) code Ansys Fluent V. 19.1 [31]. For turbulence modelling  $k-\varepsilon$  turbulence model was employed with enhanced wall treatment. While, SIMPLE algorithm [32, 33] was used for pressure-velocity coupling and all the equations were discretized using second-order formulations. In present work, single phase approach has been opted for modelling of nanofluids. Various works [34, 35] have been undertaken using similar numerical approach as it calculates fairly precise results in less computational time.

## 2.4 Boundary condition

The left side of radiator geometry is subjected to the velocity inlet condition for nanofluid. The nano fluid flows through the radiator with different flow rate having inlet temperature of  $45^{\circ}\text{C}$  (318 K). Further, hydraulic diameter of 5.3 mm and turbulent intensity of 10% was specified at the inlet. The exit of radiator is subject to pressure outlet condition, i.e. gauge pressure equal to 0 Pa. Heat flux of  $150\text{ W/m}^2\text{K}$  was applied to the radiator wall.

## 3 Validation

The present CFD model has been validated by comparing the results with previous work of Delavari *et al.* [36] (Fig. 4). The validation has been performed under turbulent regime ( $\text{Re} = 9000\text{--}23\,000$ ) for  $\text{Al}_2\text{O}_3$  based nanofluid with different particle concentrations (0.1, 0.5, and 1%). From the comparison, it is found that results obtained though CFD model has good agreement with publish results and the variation is not more than 8%. Hence, our CFD model is validated and now we can apply it to present problem.

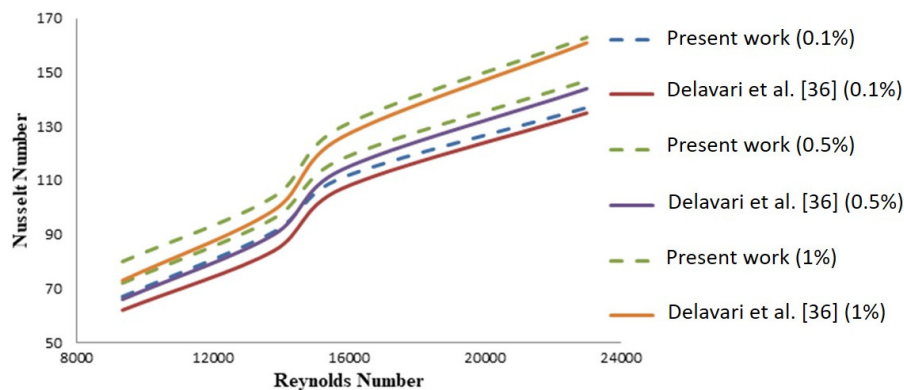


Figure 4: Comparison of Nusselt number for present work with Delavari *et al.* [36].

## 4 Result and discussion

Figure 5 shows the velocity contours in the flat tube with artificial roughness in the form of ribs. Figure 5a represents the results for the Reynolds number 9350 and Fig. 5b represents the results for the Reynolds number



23 000. The two extreme values of Reynolds number were considered for better understanding of flow physics. The artificial roughness has broken the laminar sublayer region of the boundary layer at the walls and created a recirculation zone behind the ribs. This has helped to increase the heat transfer rate in the ribbed flat tube configurations. Figure 6 shows the contours of turbulent kinetic energy (TKE) in the flat tube with artificial roughness in the form of ribs. Figure 6a represents the TKE contours for the Reynolds number 9350 and Fig. 6b represents the TKE results for the Reynolds number 23 000.

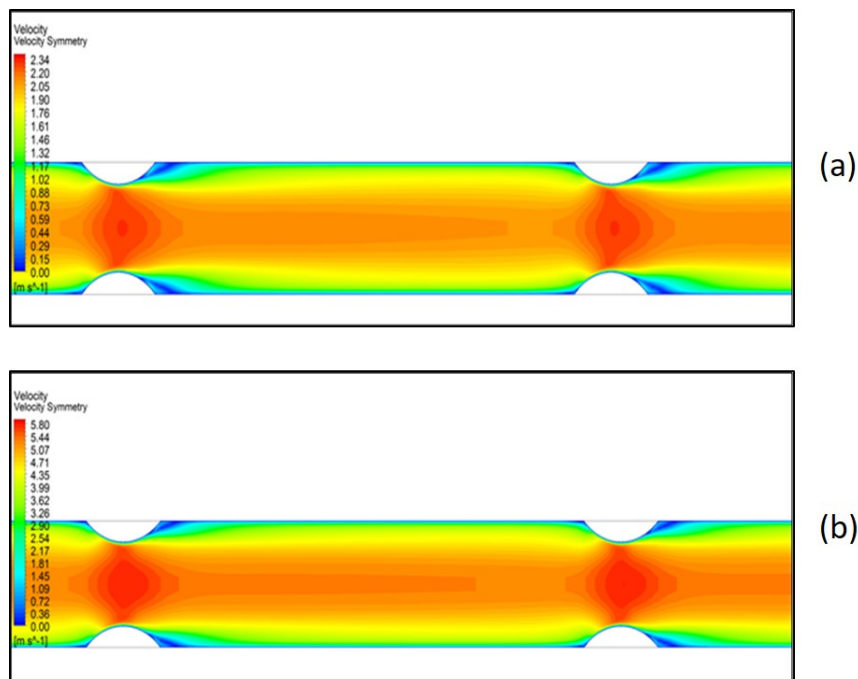


Figure 5: Velocity contours at 1% nanofluid concentration for (a)  $Re = 9350$ , (b)  $Re = 23\,000$ .

Figure 7 shows the variation of the Nusselt number with Reynolds number in a flat tube with and without artificial roughness. The results are shown for different concentration of nanofluids (0.1% to 1%) for the turbulent flow regime (Reynolds number ranging from 9350 to 23 000). It can be observed from the figure that Nusselt number increases with Reynolds number in both flat tube and ribbed tube configurations. It is also clear from the

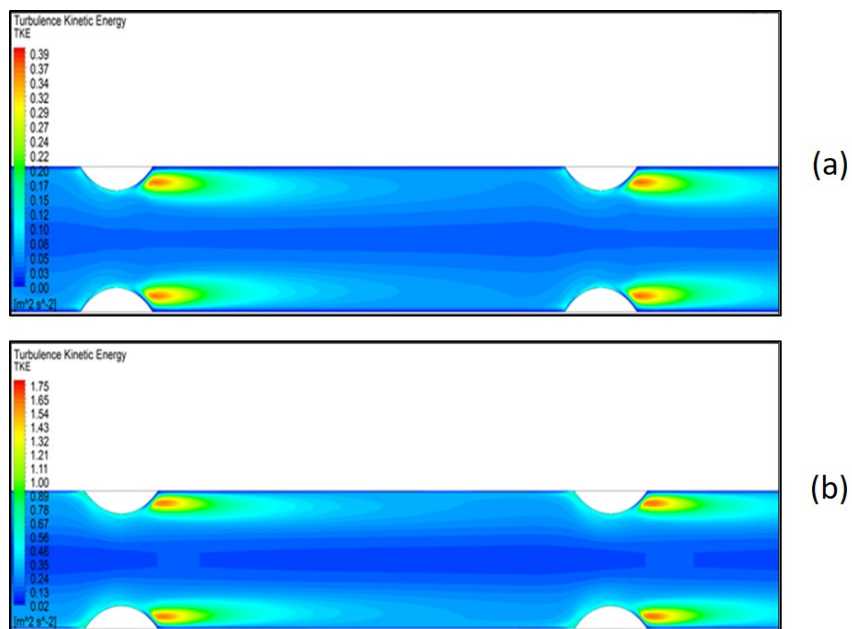


Figure 6: Turbulent kinetic energy contours at 1% nanofluid concentration for (a)  $Re = 9350$ , (b)  $Re = 23000$ .

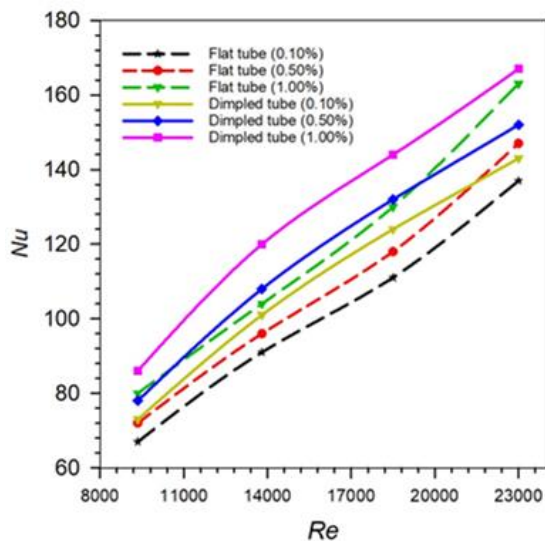


Figure 7: Nusselt number variation with Reynolds number for flat tube and dimpled flat tube configurations.

figure that the heat transfer significantly improved with the use of artificial roughness. Apart from that, it can also be observed there is the effect of nanofluid concentration on Nusselt number.

Figure 8 represents variation of percentage enhancement of Nusselt number with Reynolds number for ribbed flat tube. The results are shown for different concentration of nanofluids (0.1% to 1%) for the turbulent flow regime (Reynolds number ranging from 9350 to 23 000). It can be observed from figure that percentage enhancement in Nusselt number is more at lower Reynolds and then it decreases with increase in Reynolds number. For 1% nanofluid, the heat transfer enhancement at Reynolds 9350 is about 79% and at Reynolds 23 000 it is around 18% which is lowest. At Reynolds 15 500, all the three curves (0.1, 0.5, and 1.0%) intersect each other which indicates same enhancement at that location.

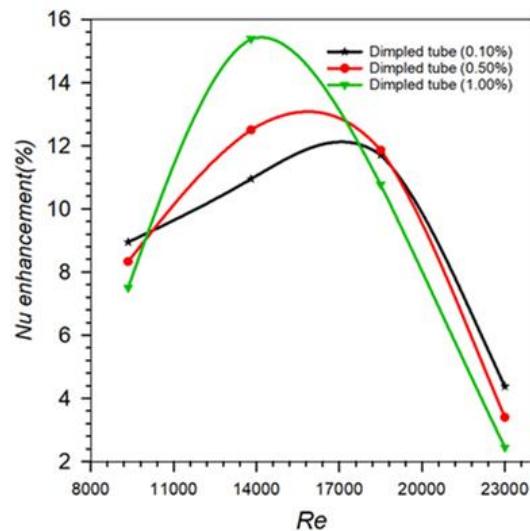


Figure 8: Nusselt number enhancement variation with Reynolds number for dimpled flat tube configurations.

The hydraulic performances for both configurations are evaluated with the help of pressure drop and pumping power requirement. Figure 9 shows the variation of the pressure drop with Reynolds number in a flat tube with and without artificial roughness. The results are shown for different concentration of nanofluids (0.1% to 1%) for the turbulent flow regime (Reynolds number ranging from 9350 to 23 000). It can be observed from the plot that ribbed tube has higher pressure drop compared to flat plat

tube. This is attributed to increase in flow obstruction. Moreover, it can also be pointed that with increase in nanoparticle concentration, the pressure drop increases. Similar trend was observed for pumping power in Fig. 10.

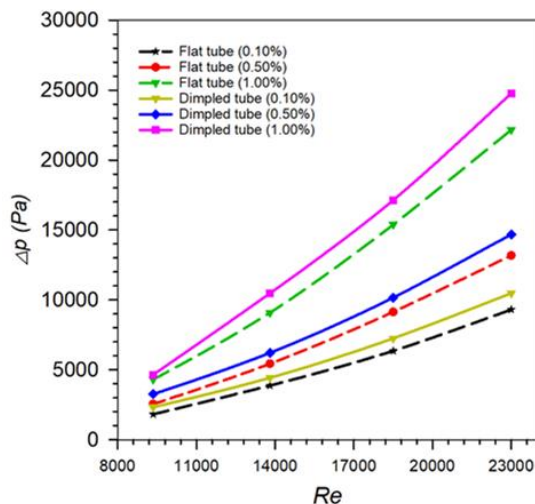


Figure 9: Variation of pressure drop with Reynolds number.

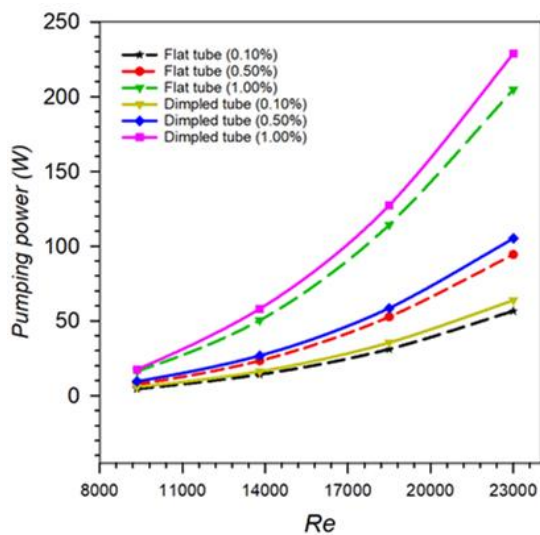


Figure 10: Variation of pumping power with Reynolds number.

## 5 Conclusions

In the present work, artificial roughness in the form of dimples were provided in the simple flat tube of the car radiator. The  $\text{Al}_2\text{O}_3$  nanoparticles in water nanofluid were used as the coolant having nanoparticle concentration varied between 0.1–1.0%. The Reynolds number of the flow was simulated in the range of 9350–23 000. The Nusselt number and pumping power for all the configurations were studied in details. Following conclusions were drawn after the study:

1. For any configuration of the flat tube (simple or dimpled) the heat transfer coefficient increases with the increase in Reynolds number.
2. The heat transfer rate also increases with increase in nanoparticle concentration from 0.1% to 1.0%.
3. On increasing the Reynolds number or nanoparticle concentration, the pumping power also increases significantly.
4. The application of artificial roughness in the form of dimples can increase the heat transfer coefficient as compared to that of simple flat tube for a particular Reynolds number.
5. For dimpled flat tube, the heat transfer enhancement is highest (79%) at Reynolds 9350 and lowest (18%) at Reynolds 23 000 for nanofluid concentration of 1%.
6. For a constant heat transfer coefficient ( $17\,000\text{ W/m}^2\text{K}$ ), the required pumping power can be reduced by up to 67% if dimples are employed in the simple flat tube at nanofluid concentration of 1%.

*Received 31 January 2022*

## References

- [1] Goudarzi K., Jamali H.: *Heat transfer enhancement of  $\text{Al}_2\text{O}_3$ -EG nanofluid in a car radiator with wire coil inserts*. Appl. Therm. Eng. **118**(2017), 510–517.
- [2] Arora N., Gupta M.: *An updated review on application of nanofluids in flat tubes radiators for improving cooling performance*. Renew. Sust. Energ. Rev. **134**(2020), 110242.

- [3] Naddaf A., Heris S.Z., Pouladi B.: *An experimental study on heat transfer performance and pressure drop of nanofluids using graphene and multi-walled carbon nanotubes based on diesel oil*. Powder Technol. **352**(2019), 369–380.
- [4] Pak B.C., Cho Y.I.: *Hydrodynamic and heat transfer study of dispersed fluid with sub-micron metallic oxide particles*. Exp. Heat Transfer **11**(1998), 151–170.
- [5] Choi S.U., Eastman J.A.: *Enhancing thermal conductivity of fluids with nanoparticles*. Argonne National Lab., 1995.
- [6] Ahmed S.A., Ozkaymak M., Sözen A., Menlik T., Fahed A.: *Improving car radiator performance by using TiO<sub>2</sub>-water nanofluid*. Eng. Sci. Technol. Int. J. **21**(2018), 996–1005.
- [7] Naraki M., Peyghambarzadeh S.M., Hashemabadi S.H., Vermahmoudi Y.: *Parametric study of overall heat transfer coefficient of CuO/water nanofluids in a car radiator*. Int. J. Therm. Sci. **66**(2013), 82–90.
- [8] Heris S.Z., Shokrgozar M., Poorpharhang S., Shanbedi M., Noie S.H.: *Experimental study of heat transfer of a car radiator with CuO/ethylene glycol-water as a coolant*. J. Disp. Sci. Technol. **35**(2014), 5, 677–684.
- [9] Maghrabie H.M., Mousa H.M.: *Thermal performance intensification of car radiator using SiO<sub>2</sub>/water and ZnO/water nanofluids*. ASME J. Thermal Sci. Eng. Appl. **14**(2022), 3, 034501.
- [10] Bhogare R.A., Kothawale B.S.: *Performance investigation of automobile radiator operated with Al<sub>2</sub>O<sub>3</sub> based nanofluid*. IOSR J. Mech. Civil Eng. **11**(2014), 3, 23–30.
- [11] Nambeesan K.P., Parthiban R., Kumar K.R., Athul U.R., Vivek M., Thirumalini S.: *Experimental study of heat transfer enhancement in automobile radiator using Al<sub>2</sub>O<sub>3</sub>/water-ethylene glycol nanofluid coolants*. Int. J. Auto. Mech. Eng. **12**(2015), 2857–2865.
- [12] Kumar N., Singh P., Redhewal A.K., Bhandari P.: *A review on nanofluids applications for heat transfer in micro-channels*. Procedia Eng. **127**(2015), 1197–1202.
- [13] Dhale L.P., Wadhve P.B., Kanade D.V., Sable Y.S.: *Effect of nanofluid on cooling system of engine*. Int. J. Eng. Appl. Sci. **2**(2015), 2, 257815.
- [14] Senthilraja S., Vijayakumar K.C., Gangadevi R.: *Experimental investigation of heat transfer performance of different nanofluids using automobile radiator*. In: Applied Mechanics and Materials. Vol. 787, 212–216. Trans Tech Publications 2015.
- [15] Chougule S.S., Nirgude V.V., Gharge P.D., Mayank M., Sahu S.K.: *Heat transfer enhancements of low volume concentration CNT/water nanofluid and wire coil inserts in a circular tube*. Energy Proced. **90**(2016), 552–558.
- [16] Singh B.P., Bisht V.S., Bhandari P., Rawat K.: *Thermo-fluidic modelling of a heat exchanger tube with conical shaped insert having protrusion and dimple roughness*. Aptisi Trans. Technopreneurship (ATT) **3**(2021), 2, 13–29.
- [17] Singh B.P., Bisht V.S., Bhandari P.: *Numerical study of heat exchanger having protrusion and dimple roughened conical ring inserts*. In: Advances in Fluid and Thermal Engineering (B.S. Sikarwar, B. Sundén, Q. Wang, Eds.), Lecture Notes in Mechanical Engineering, 2021, 151–161.

- [18] Kore S.S., Yadav R.J., Sane N.K.: *Investigation of effect of dimple depth on heat transfer and fluid flow within rectangular channel*. Procedia Eng. **127**(2015), 1110–1117.
- [19] Katkhw N., Vorayas N., Kiatsiriroat T., Nuntaphan A.: *Heat transfer behaviour of flat plate having spherical dimpled surfaces*, Case Stud. Therm. Eng. **8**(2016), 370–377.
- [20] Kumar K., Kumar S., Gupta M., Garg H.C.: *Tribological behaviour of WC-10Co4Cr coated slurry pipe materials*. Ind. Lubr. Tribol. **70**(2018), 9, 1721–1728.
- [21] Kumar K., Kumar S., Tripathi C.B., Sharma H., Prasad S.B.: *Parametric optimization of slurry erosion behaviour of brass*. Mater. Today-Proc. **26**(2020), 2, 1604–1609.
- [22] Kharkwal H., Singh S.: *Effect of serrated circular rings on heat transfer augmentation of circular tube heat exchanger*. Arch. Thermodyn. **43**(2022), 2, 129–155.
- [23] Konchada P.K., Sukhvinder B., Relangi S., Chekuri R.: *Neuro-genetic optimization of ribbed heat exchanger using entropy augmentation generation number*. Arch. Thermodyn. **41**(2020), 2, 169–184.
- [24] Datta A., Halder P.: *Thermal efficiency and hydraulic performance evaluation on Ag-Al<sub>2</sub>O<sub>3</sub> and SiC-Al<sub>2</sub>O<sub>3</sub> hybrid nanofluid for circular jet impingement*. Arch. Thermodyn. **42**(2021), 1, 163–182.
- [25] Saeed F.R., Al-Dulaimi M.A.: *Numerical investigation for convective heat transfer of nanofluid laminar flow inside a circular pipe by applying various models*. Arch. Thermodyn. **42**(2021), 1, 71–95.
- [26] Abdolhossein Zadeh A., Nakhjavani S.: *Thermal analysis of a gravity-assisted heat pipe working with zirconia-acetone nanofluids: An experimental assessment*. Arch. Thermodyn. **41**(2020), 2, 65–83.
- [27] Pak B.C., Cho Y.I.: *Hydrodynamic and heat transfer study of dispersed fluids with submicron metallic oxide particles*. Exp. Heat Transf. Int. J. **11**(1998), 2, 151–170.
- [28] Xuan Y., Roetzel, W.: *Conceptions for heat transfer correlation of nanofluids*. Int. J. Heat Mass Transf. **43**(2000), 19, 3701–3707.
- [29] Hamilton R.L., Crosser O.K.: *Thermal conductivity of heterogeneous two-component systems*. Ind. Eng. Chem. Fund. **1**(1962), 3, 187–191.
- [30] Masoumi N., Sohrabi N., Behzadmehr A.: *A new model for calculating the effective viscosity of nanofluids*. J. Phys. D Appl. Phys. **42**(2009), 5, 055501.
- [31] ANSYS Fluent Theory Guide 2009, <http://ansys.com/Products/Simulation+Technology/Fluid+Dynamics> (accessed 11 Jan. 2022).
- [32] Bhandari P., Prajapati Y.K.: *Fluid flow and heat transfer behaviour in distinct array of stepped micro pin fin heat sink*. J. Enhanced Heat Transf., **28**(2021), 4, 31–61.
- [33] Bhandari P., Prajapati Y.K., Uniyal A.: *Influence of three dimensionality effects on thermal hydraulic performance for stepped micro pin fin heat sink*. Meccanica (2022).
- [34] Zainith P., Mishra N.K.: *A comparative study on thermal-hydraulic performance of different non-Newtonian nanofluids through an elliptical annulus*. J. Therm. Sci. Eng. Appl. **13**(2021), 051027-1-10.

- [35] Zainith P., Mishra N.K.: *Experimental and numerical investigations on exergy and second law efficiency of shell and helical coil heat exchanger using carboxymethyl cellulose based non-Newtonian nanofluids*. Int. J. Thermophys. **43**(2022), 3, 1–29.
- [36] Delavari V., Hashemabadi, S.H.: *CFD simulation of heat transfer enhancement of  $Al_2O_3$ /water and  $Al_2O_3$ /ethylene glycol nanofluids in a car radiator*. Appl. Therm. Eng. **73**(2014), 378–388.